Light Metals 2012 *Edited by: Carlos E. Suarez*
TMS (The Minerals, Metals & Materials Society), 2012

THE EFFECT OF ARTIFICIAL AGING TREATMENT ON MICROSTRUCTURE AND TENSILE PROPERTIES OF AL-12.7SI-0.7MG ALLOY

Liu Fang[1], Yu Fuxiao[2], Zhao Dazhi[2], Zuo Liang[1]
[1]Key Lab. for Anisotropy and Texture of Materials (Ministry of Education), Northeastern University; No.11, Lane 3, WenHua Road, HePing District; Shenyang, Liaoning110819, People's Republic of China
[2]Department of Metal Forming, School of Materials and Metallurgy, Northeastern University; No.11, Lane 3, WenHua Road, HePing District; Shenyang, Liaoning110819, People's Republic of China

Keywords: Al-Si alloy, Extrusion, Microstructure, Tensile properties, artificial aging treatment.

Abstract

The microstructure and tensile properties of the extruded Al-12.7Si-0.7Mg alloy aged at 160°C, 180°C and 200°C were investigated. The precipitates in different aging conditions have been characterized by regular and high resolution transmission electron microscopy (TEM and HREM) aiming at understanding the strengthening mechanisms. It was shown that the alloy after T6 treatment exhibits good ductility and much higher proof strength as well as tensile strength compared to 6063 alloy in general. The results have revealed that the strength changes by altering the precipitates size and volume fraction. The strengthening was attributed to be the combining effect of particle, grain boundary and precipitation strengthening.

Introduction

For 6xxx Al-Mg-Si alloys, T4 or T6 heat treatment is in most cases an essential step in the manufacturing process. The strengthening of these alloys after heat treatment is attributed to the formation of fine precipitates resulting from the aging treatment after solution treatment [1-3]. The strengthening of wrought Al-Mg-Si alloys is based on a precipitation hardening process. The precipitation sequence in the Al-Mg-Si alloys is generally accepted as [4-6]: Supersaturated solid solution→GP zones→β″→β′→β.

Al-Si alloys with addition of Mg make a big group of cast aluminum alloys for structural purpose. Yu et al. [7] reported that the DC casting process can be used to refine primary and eutectic Si phase in hypereutectic Al-Si alloys without recourse to chemical modification and other means such as electromagnetic stirring. Further work showed that traditional metallurgical process could be used to make Mg bearing Al-Si alloys with mechanical properties comparable or even superior to that of the 6000 series alloys [8]. On this base, a complete process incorporating DC casting, hot deformation and heat treatment has been developed for manufacturing wrought Al-Si alloys as structural materials.

As in the 6xxx alloys, Mg in the wrought Al-Si alloys is taken in advantages to strength the alloys through precipitation strengthening. Although the precipitation process in Al-Mg-Si alloys has been extensively studied, the understanding of the hardening process is still incomplete, since any change in composition, processing and aging practices etc. could affect the precipitation hardening behavior [9, 10]. A good understanding of the relationship between strength and precipitation process can be favorable for artificially controlling the aging treatment and industrial purposes.

In this work, the precipitate phases of Al-12.7Si-0.7Mg alloy aged at 160°C, 180°C and 200°C were investigated by TEM and HREM in order to evaluate the effect of artificial aging treatment on microstructure and tensile properties.

Material And Methods

A DC cast Al-Si-Mg alloy(composition: 0.7 wt% Mg, 12.7wt% Si, 0.2wt% Fe and balance aluminium) billet of 110 mm in diameter was produced, without chemical modification, with a pouring temperature of 700°C and casting velocity of 3 mm/s. The billet was extruded into a profile of 4 mm in thickness at 470°C, after pre-heat-treatment at the same temperature for 2 h. The extrusion ratio is 15:1 and the ram speed was set at 10.5 mm/s during extrusion.

The specimens for tensile test were cut from the extrusion profiles along the longitudinal direction. A portion of the tensile specimens were processed to T4 (solution treatment + natural aging) and T6 (solution treatment + artificial aging) tempers. The solution treatment was performed at 540°C for 90 min in a salt bath and quenched into water at room temperature. Artificial aging was carried out at three different temperatures such as 160°C, 180°C and 200°C for a period of 1, 2, 3 h respectively in a Muffle furnace. Mechanical tests were performed on a SANS testing machine at a cross-head speed of 1 mm/min. The mechanical data for T1(as extruded), T4 and T6 conditions were the average for three specimens which were wire electric discharge machining machined corresponding to ASTM standard E8. Elongation was measured as the engineering strain at fracture.

The samples for optical observation were prepared following standard metallographic methods. An optical microscope (Leica DMI 5000M) was used for this purpose. The TEM samples were thinned to 50 μm by mechanical polishing and punched into 3 mm disks prior to the TEM experiments. Thin foils for TEM studies were twin jet electropolished in a solution of 30% nitric acid in Methanol at -20°C. Conventional TEM observations were performed using a FEI Tecnai F20 electron microscope operated at 200 KV.

Results And Discussion

General Observation Of Microstructure

Figure 1 shows the microstructures of the extruded profile on its longitudinal section after solution treatment and artificial aging. As observed in a previous work [8] it contains uniformly distributed silicon particles in the Al matrix of fine equiaxed grains. It is worthy to notice that artificial aging treatment at different temperatures did not change the size of the Si particles and the Al matrix grains are shown in Figure 1b and c. After artificial aging treatment, precipitation occurred within the matrix, but the precipitates can not be revealed by optical microscope.

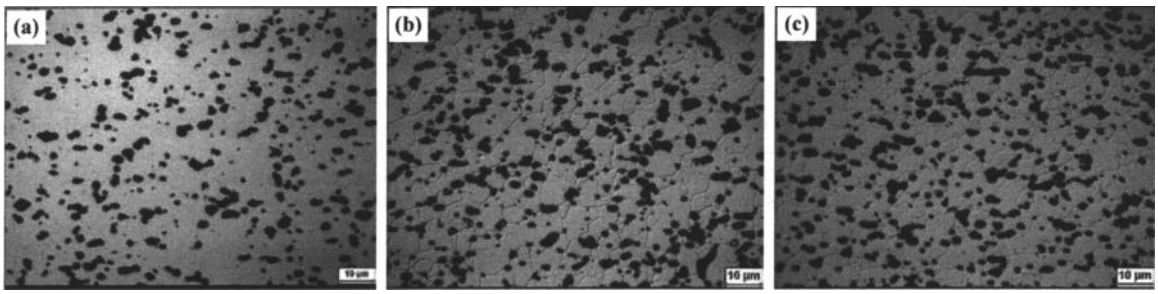

Figure 1. Optical micrographs of the alloy after heat treatment: (a) solution treatment (540°C /90 min), (b) artificial aging at 180°C for 3 h, (c) artificial aging at 200°C for 3 h.

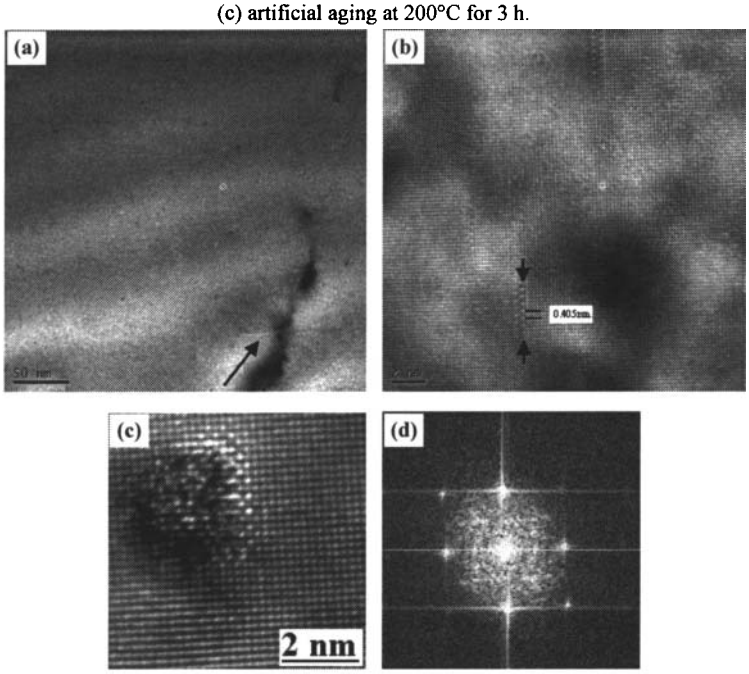

Figure 2. TEM and HREM image of the alloy aged for 3 h at 160°C, (a) TEM micrographs (B= $[001]_{Al}$) of precipitate, (b) HREM image of the needle-shaped precipitate along $[010]_{Al}$ and $[100]_{Al}$, (c) and (d) HREM and FFT of the dark spot precipitate.

TEM And HREM

Figure 2 shows TEM (B= $[001]_{Al}$) and HREM image of the alloy aged for 3 h at 160°C. Very fine dark spot precipitates were visible on the bright-field micrograph. It also can be seen that a few needle-shaped precipitates nucleated on dislocation as marked by the arrow in Figure 2a. The selective area electron diffraction (SAED) pattern obtained from the $[001]_{Al}$ zone did not show the presence of any extra diffraction spots. Figure 2b shows the HREM image of the precipitates along $[010]_{Al}$ and $[100]_{Al}$ directions. Atomic columns in the viewing direction in the image appear as bright dots. The bright dots having a spacing of 0.405 nm, are arrayed in arrow on the (200) lattice plane of the matrix. The morphology of precipitate in this alloy is similar with previous observation for GP zone [11]. HREM images of the dark spot phase with a diameter of about 2 nm are presented in Figure 2c. This precipitate shows an irregular arrangement of black-white contrast inside. The fast Fourier transformation (FFT) of the HREM image is fainter and diffuse as shown in Figure 2d. Accordingly the diffuse streaks are uncertain of crystal structure of the precipitates clearly. Extensive bright field and dark field TEM from the alloy aged at 160°C for 1 h, provided evidence of a few dark dot precipitate in the matrix.

Figure 3a shows the bright-field TEM micrograph (B=$[001]_{Al}$) of the alloy aged for 1 h at 180°C. Very fine dark dot precipitates are visible in the viewing direction. There is no obvious streak of precipitate between the diffraction spots of Al matrix after aging for 1h at 180°C. Figure 3b and c show the bright-field TEM micrographs (B=$[001]_{Al}$) of the alloy aged for 2, 3 h at 180°C, respectively. The microstructures of the Al matrix shown in Figure 3b and c are characterized by dislocations and high density very fine dot and needle precipitates. The needle-shaped precipitates are oriented along $[010]_{Al}$ and $[100]_{Al}$ directions as observed in a previous work [8]. The mean length of needle-shaped precipitates of alloy after aging for 3h is increase than that aging for 2h.

The Si content in the Mg bearing wrought Al-Si alloy in this study is much higher than that needed to form Mg_2Si, as in the case of Al-Mg-Si alloys in general. The aging temperature of 180 °C and 200°C used in this study are the temperature at which the needle-shaped precipitate β″ along $<001>_{Al}$ is formed in Al-Mg-Si

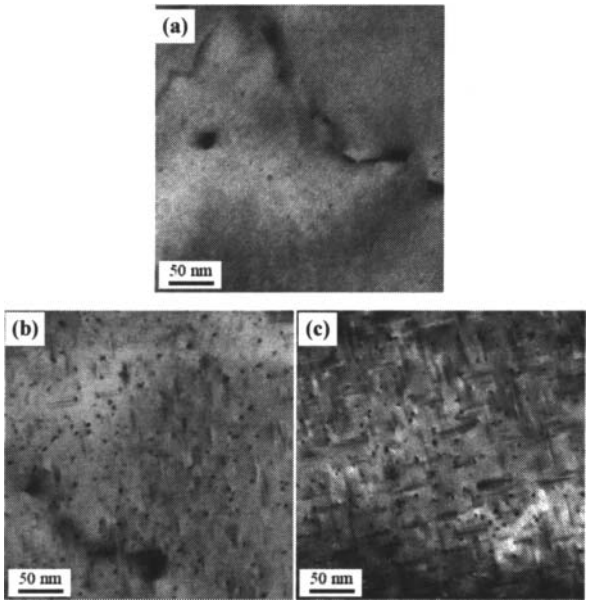

Figure 3. TEM images of the Al-12.7Si-0.7Mg alloy at different treatment conditions: (a) aged at 180°C for 1 h, (b) aged at 180°C for 2 h, (c) aged at 180°C for 3 h.

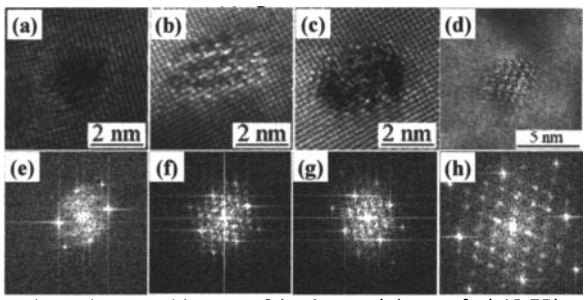

Figure 4. HREM images of the dot precipitates of Al-12.7Si-0.7Mg alloy(a) aged at 180°C for 1h, (b) and (c) aged at 180°C for 2h, (d) aged at 180°C for 3h, (e) to (h) the Fourier transform of the HREM image in (a) to (d), respectively.

alloys [2,10]. In the case of the Al-Mg-Si alloys with excess of Si, previous TEM works showed that the excess Si does not alter the precipitation sequence, structure and lattice parameters of different metstable precursors, but rather results in modification of the composition and density of particles [9,10]. Nevertheless, Investigators considered that needle-shaped precipitate is β″ and the dark dots should be the cross sections of the needles along $[001]_{Al}$ [2,4,5,10,11]. The cross section of the dark dot precipitates were investigated in detail in this work.

HREM image of the dark dot precipitate of the alloy aged at 180°C for 1 h with a diameter of about 2 nm is presented in Figure 4a. The cross section shape of the precipitates is generally either nearly circular or circular with one or more bulges. The FFT pattern of the HREM image of the phase in the matrix is fainter and diffuse. Figure 4b and c show the typical HREM images of the dark dot precipitate for the alloy aged at 180°C for 2 h. The cross section shape of the dark dot precipitate shows an ellipsoidal-shaped image that is 2-3 nm in size. The precipitate shows parallelogram-shaped image for the alloy aged at 180°C for 3h that is 3-4 nm in size as shown in Figure 4d. The other precipitates are observed as shown in Figure 4b and c. The appearance of the precipitates in Figure 4b to d and the streaks on the FFT are in agreement with previous observations for β″ precipitates [2].

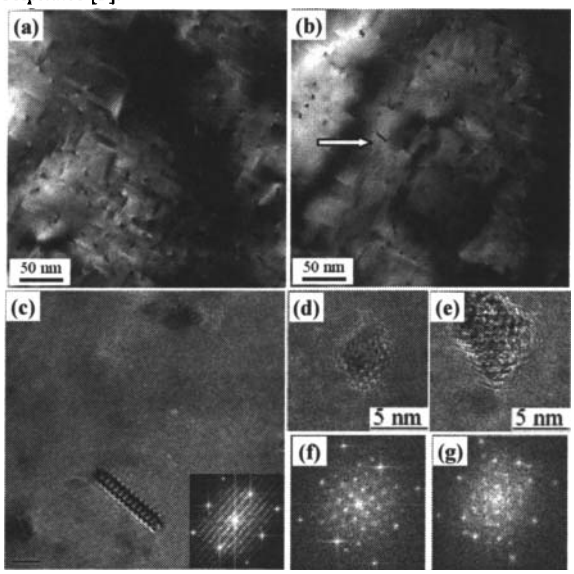

Figure 5. (a) and (b) TEM image of the alloy aged at 200°C for 1 h, (c) HREM image of the lath precipitate, the corresponding the FFT pattern is inserted into the HREM image, (f) and (g) the Fourier transform of the HREM image in (d) to (e), respectively.

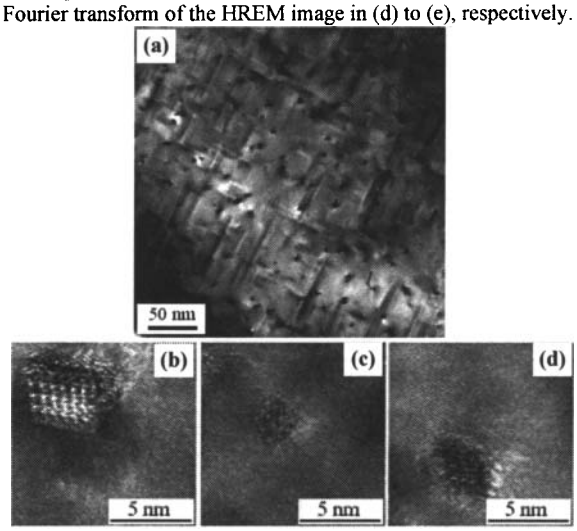

Figure 6. TEM and HREM images of the alloy aged for 3 h at 200°C, (a) TEM image, (b) to (d) HREM image of dark dot precipitates.

Figure 5 shows TEM (B=$[001]_{Al}$) and HREM image of the alloy aged for 1 h at 200°C. The observed needle-shaped precipitate are aligned in the $[010]_{Al}$ and $[100]_{Al}$ in the matrix. The mean length of the precipitates is 28 nm. The dark dot precipitates observed form the $[001]_{Al}$ has larger size compare to aging at 180°C. Figure 5c shows the HREM micrograph of a lath shaped precipitate as marked by arrow in Figure 5b. The angle between the long face of the precipitate cross-section and the $[100]_{Al}$ is about 10 degrees. The morphology and orientation are very close

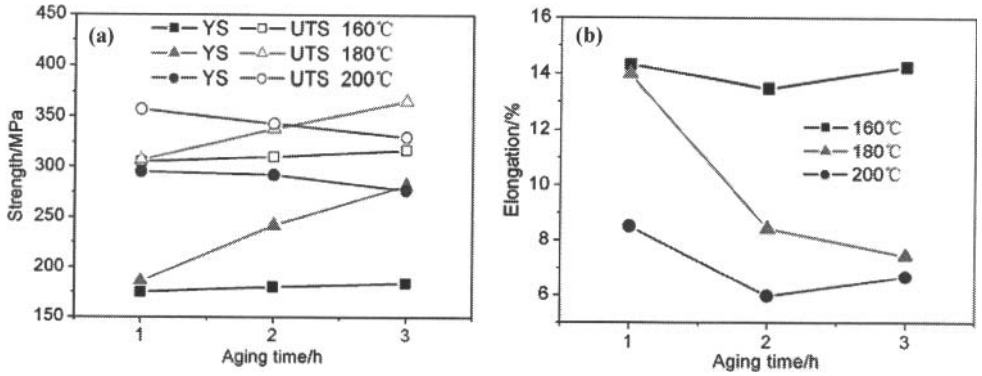

Figure 7. Mechanical properties curves of the Al-12.7Si-0.7Mg alloy aged in different aging treatment conditions.

to the structure of the B precipitate that was reported by Dumolt et al. [12], therefore this precipitate is considered to be B'. Careful HREM observations in Figure 5d to e of the alloy, which were revealed that the precipitate different size and morphology, indicated that the predominant precipitate phases after aging for 1h at 200°C is also β″ precipitates.

Figure 6 shows TEM (B=$[001]_{Al}$) and HREM image of the alloy aged for 3 h at 200°C. The TEM image is quite similar to the alloy aged for 3 h at 180°C. The needle-shaped precipitate lie along $[010]_{Al}$ and $[100]_{Al}$ has grown to larger size compare toaging at 180°C, now being about 50-100nm in length as shown in Figure 6a. Figure 6b to d shows the HREM images of dark dot precipitates. Dark dots have different size and shape. After aging for 3 h at 200°C, the dark dot precipitates are mainly β precipitates through viewing the morphology and streak on the FFT of the precipitates.

Tensile Properties

Table I. Mechanical properties of the Al-12.7Si-0.7Mg alloy in different treatment conditions

Alloy state	YS (MPa)	UTS (MPa)	Elongation(%)
T1	108	190	15.03
T4	151	285	14.08

Table II. Mechanical properties of extruded 6063 alloys (GB/T 6892-2000) [13]

Alloy state	YS (MPa)	UTS (MPa)	Elongation(%)
T4	65	130	12
T6	180	205	8

Table I lists the mechanical properties of the Al-12.7Si-0.7Mg alloy treated in T1 and T4 conditions and Table II gives the mechanical properties of 6063 alloy according to China National Standard, GB/T 6892-2000 [13] for comparison. The ultimate tensile strength (UTS) and yield strength (YS) of the Al-12.7Si-0.7Mg alloy in T1 condition (190MPa and 108MPa) is much higher than that (130MPa and 65MPa) of 6063 alloy in T4 condition as shown in Table I and Table II. As previous study [8], the strengthening mechanisms of Al-12.7Si-0.7Mg alloy in T1 condition are from grain boundary and particulate strengthening.

Comparisons of the effect of the aging treatment on tensile properties for Al-12.7Si-0.7Mg alloy are shown in Figure 7. No significant increase was found in strength of the alloy aged at 160°C accompany with increasing the aging time. The YS of the alloy aged at 160°C is equivalent to 6063 alloy in T6 condition. The UTS and elongation of the alloy is much higher than 6063 alloy in T6 condition. The strength of alloy aged at 160°C is higher about 20MPa than that of the alloy in T4 condition. The increased mechanical strength of the alloys originates mainly from the dark dot precipitates. The mechanical properties of the alloy, a continuous and pronounced increase in strength with the increase in aging time from 1 h to 3 h at 180°C is observed as seen. It has been found that the strength and ductility of the alloy were clearly affected by the evolution of precipitate morphology. The predominant precipitate phase after aging for 2 h and 3 h at 180°C is the needle and the dot precipitate (Figure 3b and c). The precipitates are thus considered to be responsible for increase in the strength in this alloy. The strength the alloy decreased gradually aged at 200°C as a result of overaging. The alloy after aging at 200°C for 1 h exhibits good ductility and much higher yield strength as well as ultimate tensile strength compared to 6063 alloy in T6 condition. The elongation of the alloy aged at 200°C hold for 2 h and 3 h is lower than that of (8%) 6063 alloy in T6 condition. The TEM and HREM image shown in Figure 5 and Figure 6 indicate that the precipitate has grown to larger size compare to aging for other aging treatment. In the over-aged conditions, precipitates coarsen via Ostwald ripening. Clearly, the hardening behavior of the Al-12.7Si-0.7Mg alloy depends on the size, distribution and number density of precipitates.

The fact that the mechanical properties of the Mg bearing Al-Si alloys aging at 160°C and 180°C can be made comparable or even superior to that of the 6000 series alloys through traditional metallurgical process is attractive from the viewpoint of industrial application of the Al-Si alloys.

Conclusions

1. The Al-12.7Si-0.7Mg alloy after T6 treatment exhibits good ductility and much higher yield strength as well as ultimate tensile strength compared to 6063 alloy in T6 condition.
2. The predominant precipitate phase aged at 180°C and 200°C for different time is β″ viewed cross-section of these precipitate along $[001]_{Al}$ by HREM.
3. The aging hardening process could be used to make Mg bearing Al-Si alloys with mechanical properties comparable or even superior to that of the 6000 series alloys.

Acknowledgments

This work was supported by the National Natural Science Foundation of China under grants Nos. 50734006 and 50771030 and by the Ministry of Science and Technology of China under grants Nos. 2007AA03Z516, 2008AA030701 and 2009BAE80B01. The authors thank Mr. Bian Weimin for his assistance in the area of transmission electron microscopy.

References

1. J. H. Chen et al., "Atomic Pillar-Based Nanoprecipitates Strengthen AlMgSi Alloys," *Science,* 312 (2006), 416-419.
2. S. J. Andersen et al., "THE CRYSTAL STRUCTURE OF THE β″ PHASE IN Al-Mg-Si ALLOYS, " *Acta Mater.,* 46 (1998), 3283-3298.
3. C. D. Marioara, et al., "Atomic model for GP-zones in a 6082 Al-Mg-Si system, " *Acta Mater.,* 49 (2) (2001), 321-328.
4. G. Thomas, B. Sc., and Ph. D., "The Aging Characteristics of Aluminium Alloys Electron-transmission Study of Al-Mg-Si Alloys, " *J. Inst. Metals,* 90 (1961-1962), 57-63.
5. M. H. Jacobs, "The structure of the Metastable precipitates Formed During Aging of an Al-Mg-Si Alloy, " *Phil. Mag.,* 26 (1972), 1-13.
6. G.A. Edwards, et al., "The precipitation sequence in Al-Mg-Si alloys, " *Acta Mater.,* 46 (11) (1998) 3893-3904.
7. Yu Fuxiao, Li Yinfeng, and Cui Jianzhong, "Banded structure in the semi-continuously DC cast Al-15Si alloy, " *Trans. Indian Inst. Met.,* 58 (4) (2005), 591-596.
8. Liu Fang, et al., "Microstructure and mechanical properties of an Al-12.7Si-0.7Mg alloy processed by extrusion and heat treatment, " *Mater. Sci. Eng. A,* 528 (2011) 3786-3790.
9. A.K. Gupta, D.J. Lloyd and S.A. Court., "Precipitation hardening in Al-Mg-Si alloys with and without excess Si, " *Mater. Sci. Eng. A,* 316 (2001), 11-17.
10. M.F. Miao, D.E. Laughlin, "Precipitation hardening in Aluminium alloy 6022, " *Scr. Mater.,* 40 (7) (1999) 873-878.
11. Kenji Matsuda et al., "High-Resolution Electron Microscopy on the Structure of Guinier-Preston Zone in an Al-1.6Mass Pct Mg_2Si alloy, " *Metallurgical and Materials Transactions A,* 29 (1998),1161-1167.
12. Dumolt, S. D. et al., "Formation of a modified β″ phase in aluminum alloy 6061, "*Scr. metall.,* 18 (1984) , 1347-1350.
13. Chunsheng Li, Debin Huang, *Metallic Materials Handbook,* （China, Beijing: Chemical Industry Press, 2005） , 829.